

Original Article

An Unconventional Circularly Polarized Cylindrical Dielectric Resonator Antenna for GPR Applications

A. Ushasree¹, Vipul Agarwal², M. Satyanarayana³

^{1,2}Department of ECE, Koneru Lakshmaiah Education Foundation, AP, India

³Department of ECE, MVGR College of Engineering, AP, India

¹Department of ECE, Gokaraju Rangaraju Institute of Engineering and Technology, Hyderabad, India

¹Corresponding Author : ushasreemishra@gmail.com

Received: 14 March 2023

Revised: 20 April 2023

Accepted: 15 May 2023

Published: 29 May 2023

Abstract - An ultra-wideband (UWB) antenna is designed, which is fed by a coplanar waveguide along with Dielectric Resonator Antenna (DRA) is discussed. The patch of ultra-high-frequency antenna structure comprises many full circles and half circles, rearranging the two focal point orientation and dimension of radius such that the antenna works in ultra-wideband frequency range and a rectangular slot in the middle of the antenna patch to change the orientation of current distribution. The antenna is resonating at 8.9GHz with a reflection coefficient (S_{11}) of -15.39dB, Gain is negative at resonating frequency, and Polarization at resonating frequency is linear. The proposed antenna is designed by mounting Cylindrical Dielectric Resonating Antenna (CDRA) on the rectangular slot made on the patch. By mounting a cylindrical DRA structure on the patch, the antenna is resonating at 3.6 GHz with a reflection coefficient (S_{11}) value - 22.54dB, achieving a Gain of 3.44dB at resonating frequency. The Polarization achieved by placing cylindrical DRA is circular Polarization which is more useful in Ground Penetrating Radar (GPR) applications. The proposed antenna is practically designed, and performance characteristics are measured and verified with simulation results.

Keywords - Ultra wide band, Coplanar waveguide, Dielectric resonating antennas, Polarization and ground penetrating radar.

1. Introduction

Ground Penetrating Radar (GPR) is a noncorrosive tool for non-intrusive exploration [1]. GPR is a geographical practice that can be used to examine and record the dielectric properties of the underground [2]-[3]. The working of the GPR system mainly depends on the antenna employed. The antenna transmits electromagnetic signals into the earth's subsurface and receives the reflected signals, which can be viewed on the display unit. The reflected signal depends on the contrast of materials[4]-[5]. Reflectivity depends on different underground materials like dry sand, wet sand, water, rocks, ice, etc., with different dielectric constants[6].

The frequency of operation of the antenna and depth of penetration of radar signal from the antenna plays a significant role in detecting the pollutants beneath the ground [7]. To confine the range, outline, direction, and electrical properties of hidden things in GPR, Polarization is a significant concern in antenna design. These polarizations, dependent on scattering distinctiveness, can be used to categorize different classes of targets for the finest object recognition.

On the contrary, ignoring the polarization aspects of GPR can lead to a false evaluation of the Physical outline and inclination of objects in the field, especially in the case of buried objects where there is a chance of interpretation missing. The direction of magnitude can strongly impact the resulting image. Even elementary features, like immersion layers, can mask the individual objects that are the target of a survey [8].

Generally, the GPR frequency range of operation is between 10MHz to 3GHz. However, if the antennas are designed at the wide band or ultra-wideband range, the image's resolution will be superior, which helps to study the properties of buried objects perfectly [9].

2. Literature Survey on DRA

There are many different models of antenna designed for GPR applications. In this paper antenna design is accomplished with Dielectric Resonator Antenna (DRA) which has many advantages like high Q factor, low insertion loss, high dielectric constant, no conduction losses and compact in size, etc. [2][23-29].



Table 1. Literature survey

Sl. No.	Resonant Frequency	S11	Polarization	Gain
[13]	857MHz-885MHz	-30dB to -40dB	LP	3.75dBi
[14]	2.34GHZ	-28dB to -35dB	LP &CP	positive
[15, 16]	2GHz	-30dB to -40dB	CP & LP	13.3dBi
[17]	5.2GHz	-30dB to -40dB	LP	4.1dBi
[18]	60GHz	-30dB	LP	8.6dBi
[19]	2.65GHz	-20dB to -22dB	LP	0.62dB
[20]	2.31 GHz -2.61GHz	<-10dB	LP	-
[21]	2.82GHz-3.83GHz	<-10dB	CP	5.5dBi
[22]	6.125GHz	-26dB	LP	10.14dBi

Table 2. Comparison of feeding techniques

Characteristics	Coaxial Probe Feeding	Microstrip Feeding	Aperture Feeding	CPW Feeding
Bandwidth	Better	Good	Fair	Better
CP bandwidth	Difficult	Easy	Better	Better
Polarization purity	Poor	Good	Good	Good
Impedance Matching	Easy	Easy	Easy	Easy
Ease of Fabrication	Soldering and Drilling Required	Easy	Alignment Required	Alignment Required
Reliability	Poor	Better	Good	Good
Configuration	Non-polar	Coplanar	Planar	planar

Over the last three decades, the geometrical models of DRA have been studied. The following table shows therecent performance parameters of different geometric models of antenna designed using DRA. From the above Table 1. It can be concluded that DRA gives suitable performance parameters. The frequency of operation of CDRA is given by

$$f_r = \frac{c}{2\pi r \sqrt{\epsilon_{DRA}}} \left[1.71t \frac{r}{h} + 0.1578 \left(\frac{r^2}{h} \right) \right]$$

Where, r = radius of CDRA
 h = height of CDRA
 c = velocity of light (3x10^8m/sec)
 ε = dielectric constant of CDRA

The above equation is valid for hybrid mode. CDRA also supports TE and TM modes, resonant frequencies are given by,

$$f_{TE_{n\pi m}} = \frac{c}{(2\pi \sqrt{\epsilon_r \mu_r})} \sqrt{\left(\frac{X_{np}}{a}\right)^2 + \left(\frac{(2m+1)\pi}{2h}\right)^2}$$

$$f_{TM_{n\pi m}} = \frac{c}{(2\pi \sqrt{\epsilon_r \mu_r})} \sqrt{\left(\frac{X_{np}}{a}\right)^2 + \left(\frac{(2m+1)\pi}{2h}\right)^2}$$

There are different feeding techniques for CDRA; among them, the Coplanar waveguide feeding technique has better characteristics. The following table shows the comparison of various feeding techniques.

3. Existing Antenna Design-1

The ultra-high frequency antenna structure patch comprises many full circles and half circles. Rearranging the two focal point orientation and dimension of radius such that the antenna works in ultra-wideband frequency range and a rectangular slot in the middle of the antenna patch to change the orientation of current distribution [5]. The distance of the coplanar waveguide (s₀₂) must be attuned to the suitable value such that an accurate match is achieved when s₀₂ = 0.2mm antenna gets the exceptional resonance. The radiation patch incorporates many half-circles and circles that go beyond each other. To make the antenna work in an ultra-wideband frequency range, the radius of circle (a) and the radius of half circle(b) are adjusted.

Table 3. Dimensions of the proposed antenna

W ₂	28
L ₂	26
W _{f2}	1.5
W ₁₂	3
a	8.2
b	12.2
m	15
n	0.2
L ₀₂	10.3
S ₀₂	0.2
H	1.6
DRA	8x8

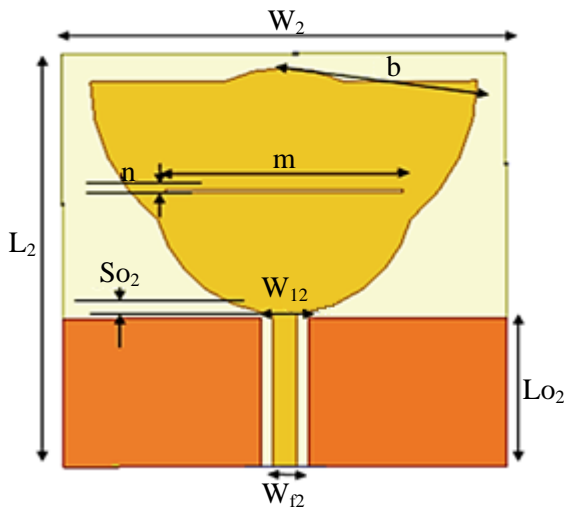
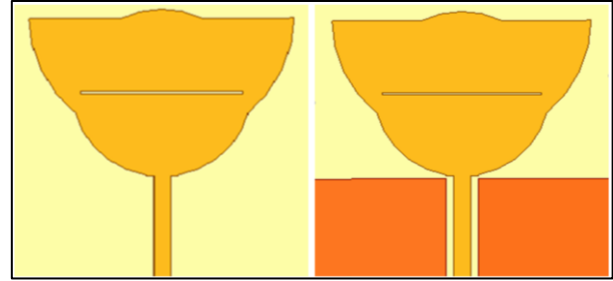


Fig. 1 Patch antenna with coplanar waveguide feed

By increasing the value of ‘a’, the reflection coefficient in the frequency band moves down considerably. When the value of ‘a’ is 8.2mm, the antenna gets the optimal resonance. In order to change the distribution of current, a rectangular slit is made so that a notch function is achieved. The length of the gap mainly exaggerates the band-notched ‘m’. As the value of ‘m’ increases, the band-notched noticeably shifts to the left. Finally, the value of ‘m’ is set at 15mm, so there will not be any problem with interference with other frequency bands.

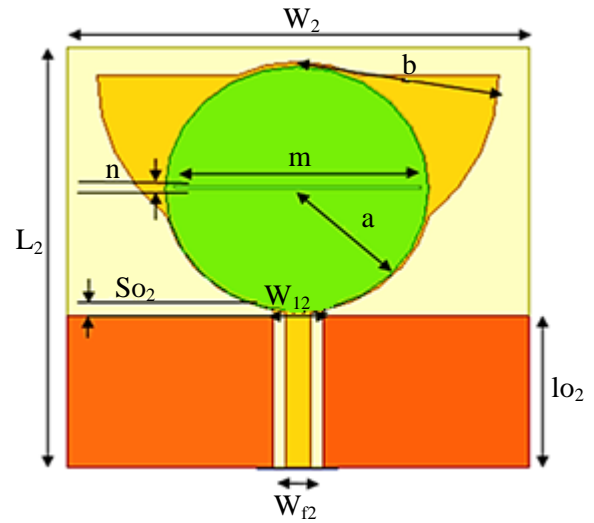
4. Results Discussion for Existing Design

The performance characteristics of the existing antenna design are analyzed. The reflection coefficient is - 15.39dB at resonance frequency 8.9GHZ. Linear Polarization is observed at the resonant frequency by the axial ratio graph.

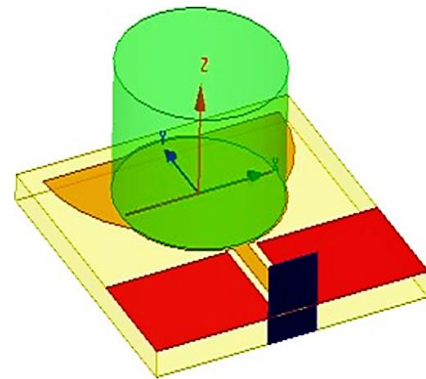


(a) Stage-1

(b) Stage-2



(c) Stage-3



(d) Side view

Fig. 2 Proposed antenna design process with DRA

The Gain at the resonant frequency is negative. Since the Gain is negative, it is not used in GPR applications as the signal cannot penetrate more distance.

5. Proposed Antenna Design-2

To overcome the disadvantages of the existing design, the proposed design uses CDRA, which is mounted on the rectangular slot, to achieve better performance results (discussed in later sections). The proposed antenna design is shown Figure 2. The dimensions of the proposed antenna are shown in Table 3.

Table 4. Performance parameters of DRA of different sizes

Parameters	With DRA Cylinder height =22mm, radius =6.5mm	With DRA cube 5*5*2	With DRA cube 6*6*4
S11(dB)	-17.96	-17.8	-19.14
Frequency (GHz)	10.9	8.8 to 9.1 GHz	8.73 to 9.16GHz
VSWR	1.28	1.29	1.24
Gain(dB)	9.993	-1.83	-1.2498
(By Axial Ratio) Polarization	Linear Polarization	Linear Polarization except in 8.8 to 9.1 GHz	Linear Polarization, except in 8.73 to 9.16 GHz

The HFSS software verified the simulation results, and the antenna was fabricated. Different types of DRA are available, as shown below [10]-[13]. The simulation is carried out considering cube and cylinder DRA of different sizes. Table 4 shows the performance parameters of different CDRA and cube DRA sizes, which shows negative Gain for cube DRA and positive Gain for CDRA. The analysis was carried out considering only CDRA.

6. Simulation Results of CDRA of Different Sizes

The Cylindrical Dielectric Resonator Antennas mounted on the patch have experimented with dimensions like XxY, where X is DRA’s radius, and Y is DRA’s radius. The first case considered here is a change in X value, i.e. for different radius values like X=4, 5, 6, 8, 22. The performance characteristics are verified in all the cases. Similarly, the second case is changing the height of DRA Y=4, 5,6,7&8. The performance characteristics are verified. In this section, the performance of the proposed antenna is simulated and analyzed using HFSS.

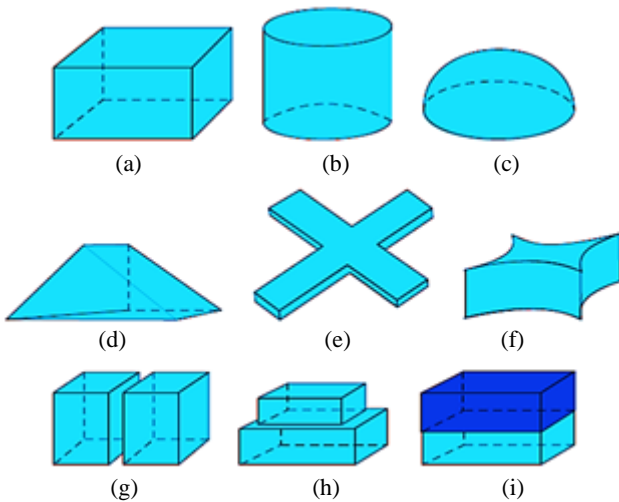


Fig. 3 Different models of DRA

The simulation results are compared to check the superiority in design for the existing antenna design (without DRA) and the Proposed antenna design (with Cylinder DRA). The essential parameters investigated for the analysis, namely Return loss or Reflection Coefficient(S11), Gain, Radiation Pattern, Axial ratio, Radiation efficiency and VSWR, are plotted for both antennas.

6.1. Reflection Coefficient

This parameter describes how much of an electromagnetic wave is reflected by an impedance discontinuity in the transmission medium. Generally, the reflection coefficient value should be a minimum of -10dB, representing 1/10th power reflected, so the lesser the negative value will be the S₁₁ value. The simulation results for the different dimensions of CDRA are analyzed by changing the radius and height of the CDRA. The CDRA considered here are 5x8, 6x8, 7x8, 8x8, 22x6.5, 8x4, 8x5, 8x6 and 8x8 which show variation in radius and height. The simulation results are shown in Figure 4(a) and Figure 4(b), which depict DRA with 8x8 has better performance results. The simulation results of the two designs are observed as -19.39dB at 8.9GHz without DRA and -23.5dB at 3.6GHz with cylindrical DRA of dimensions 8x8. The simulation graphs are shown in the following Figure 4(c).

6.2. VSWR

The parameter indicates the amount of contradiction between an antenna and the feed line connecting to it. The maximum and minimum value of VSWR is ∞ one, respectively. For most Antenna applications, the suitable VSWR value is less than 2. The two designs’ simulation results are observed at 1.240 at 8.9GHz without DRA and 1.33 at 3.6GHz with cylindrical DRA. The simulation graphs are shown in Figure 5.

6.3. Gain

It is the product of the efficiency and directivity of the antenna. This parameter depicts the input power conversion to radio waves directed in a specific direction by the antenna.

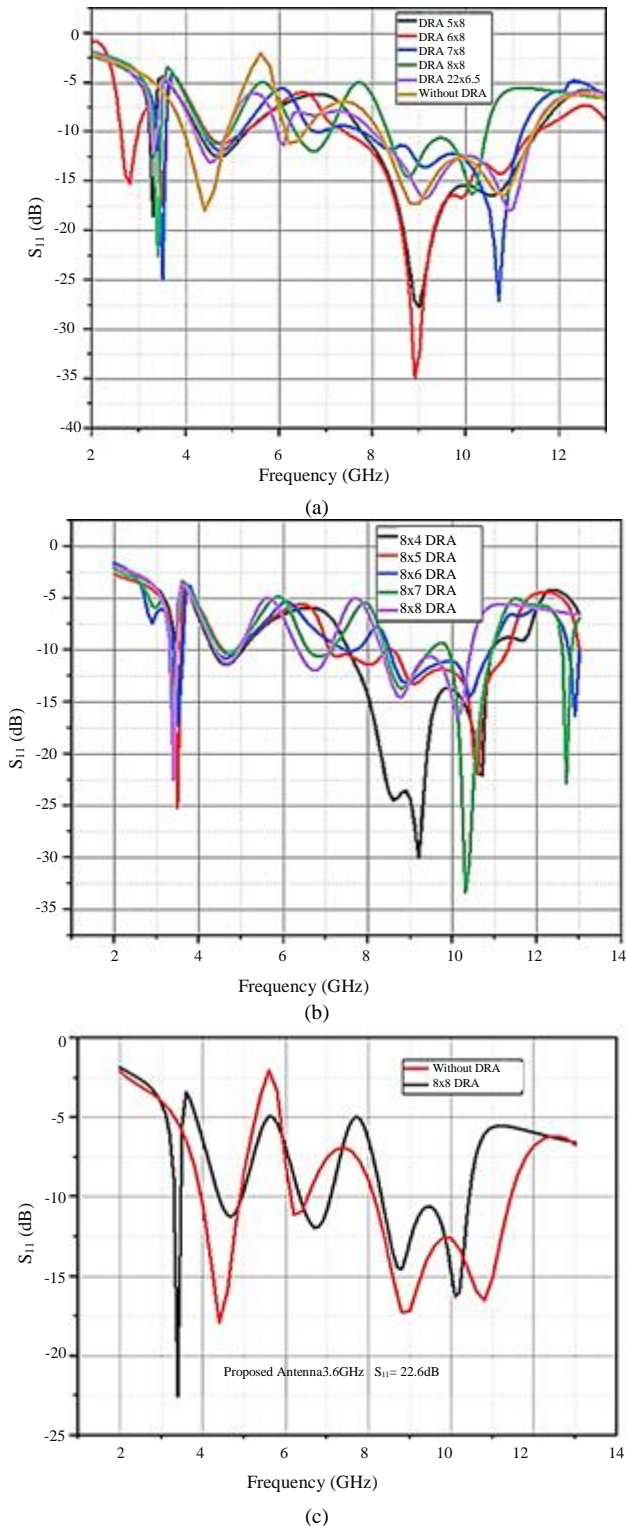


Fig. 4 Reflection coefficient graph with and without DRA(a,b,c)

Various parameters affect the antenna's Gain, like antenna substrate, antenna feed mechanism, frequency of operation, loading of materials on antenna, etc.

The two designs' simulation results are -3.059dB at 8.9GHz without DRA and 6.68 at 3.6GHz with cylindrical DRA. The simulation graphs are shown in Figure 6, where it is observed that other dimensions of DRA gain are negative.

6.4. Axial Ratio

It is the ratio of electrical fields along the orthogonal axis. There are three types of Polarization (i) Linear Polarization which indicates Axial ratio= ∞ (ii) Circular Polarization which indicates Axial ratio=1 (iii) Elliptical Polarization which indicates Axial ratio ranging from 1 to ∞ . Among different types of Polarization, circular Polarization is preferred.

The simulation results of two designs are observed where linear Polarization is achieved without DRA at 8.9GHz, and circular Polarization is achieved with cylindrical DRA at 3.6GHz. The simulation graphs are shown in Figure 7(b).

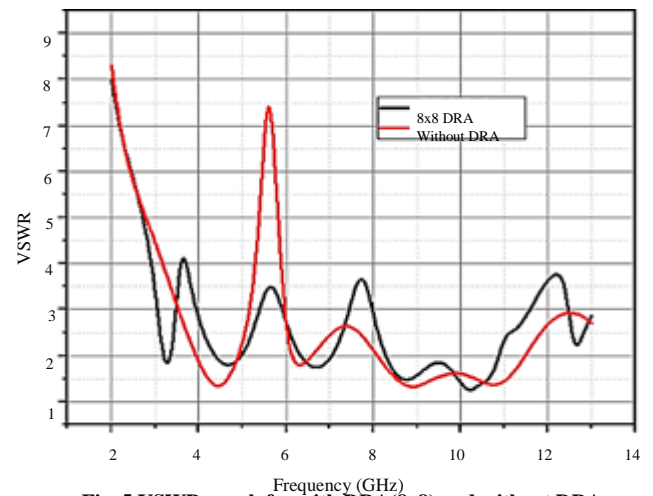


Fig. 5 VSWR graph for with DRA(8x8) and without DRA

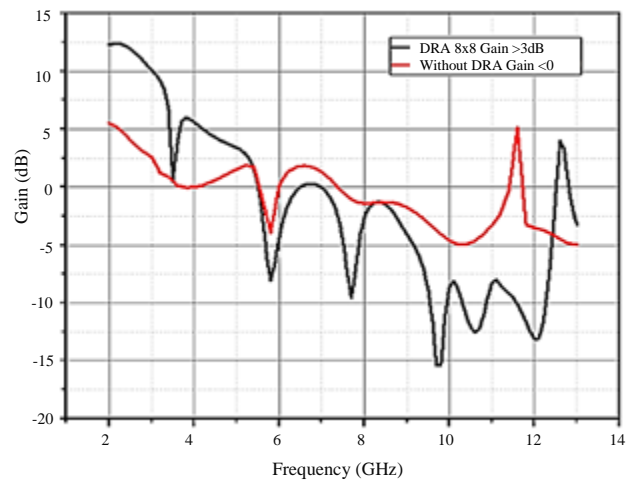


Fig. 6 Gain plot with DRA (8x8) and without DRA

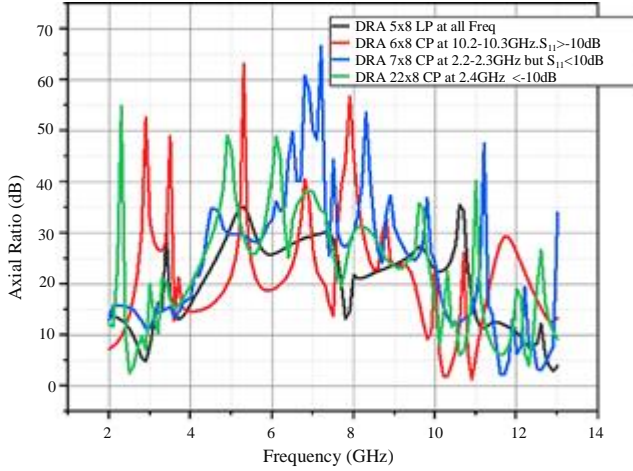


Fig. 7(a) Axial ratio plot with DRA

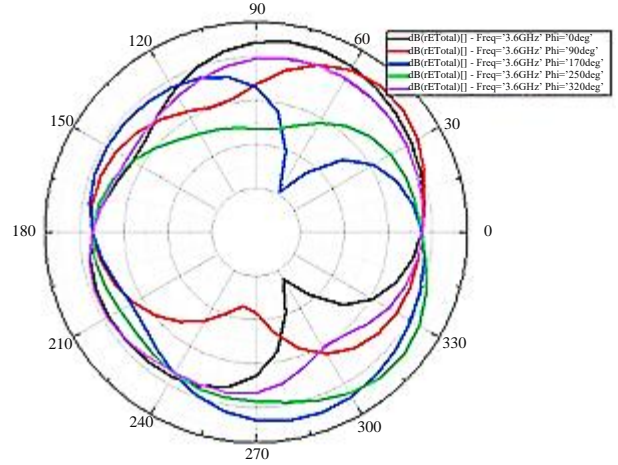


Fig. 9(a) Radiation pattern with DRA

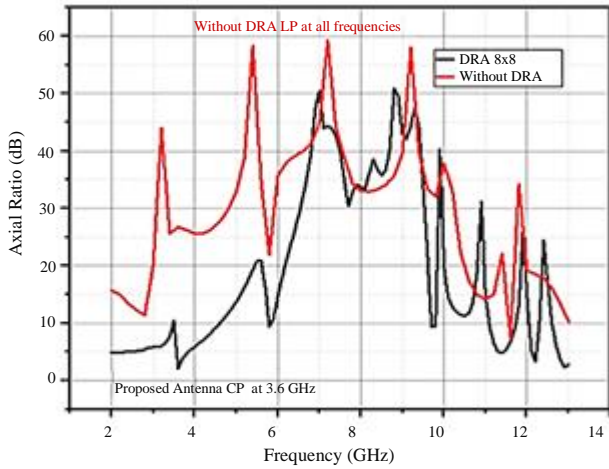


Fig. 7(b) Axial ratio plot without DRA

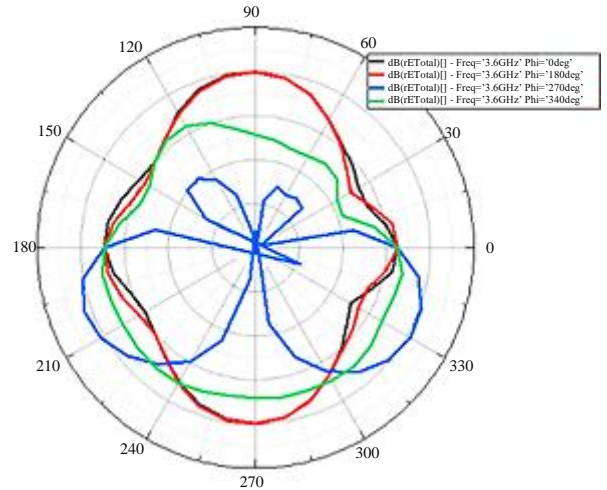


Fig. 9(b) Radiation pattern without DRA(b)

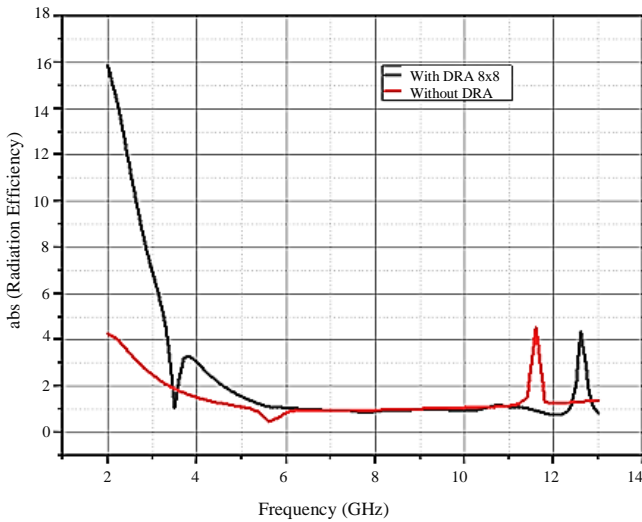


Fig. 8 Radiation efficiency with and without DRA plot

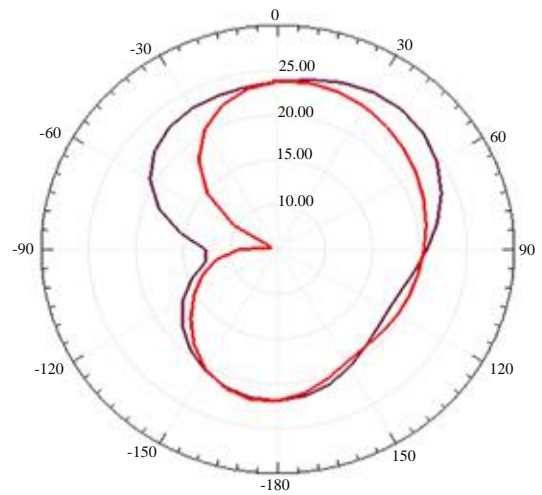


Fig. 10(a) LHCP and RHCP at 3.6GHz 0 degrees

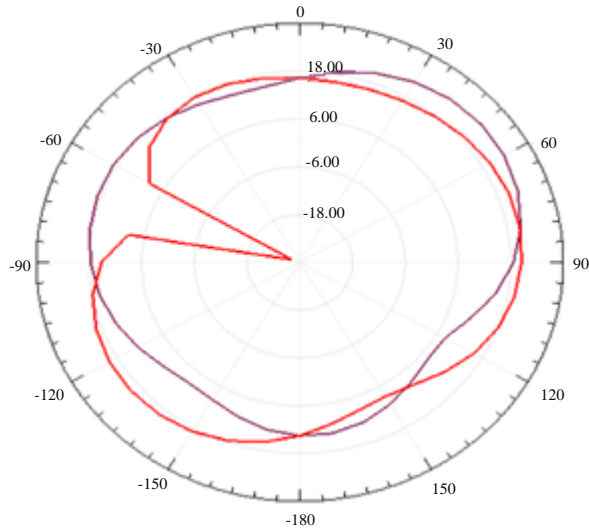


Fig. 10(b) LHCP and RHCP at 3.6GHz 90 degrees

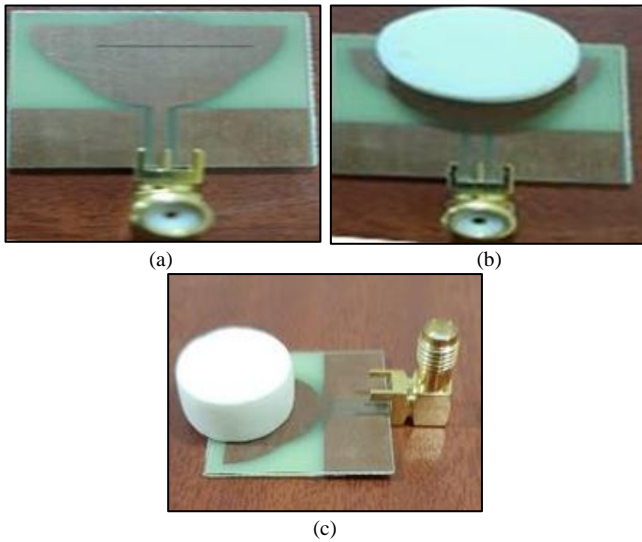


Fig. 11 Overview of fabricated antenna



Fig. 12 Testing fabricated antenna in VNA



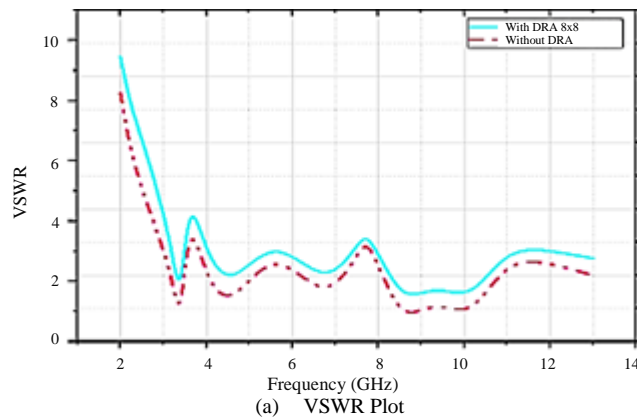
Fig. 13 Testing antenna in Anechoic Chamber

6.5. Radiation Efficiency

The ratio of the total power radiated by an antenna to the net power accepted by the antenna from the connected transmitter. The simulation results of Figure 8 show that the antenna designed with CDRA 8x8 has better efficiency than without DRA.

6.6. Radiation Pattern

The antenna pattern (or radiation pattern) is the geometric pattern of the relative strengths of the field emitted by the antenna. The radiation pattern reflects the ‘sensitivity’ of the antenna in different directions, and knowledge of this allows the antenna to be orientated in the optimum direction to ensure the required performance.



(a) VSWR Plot

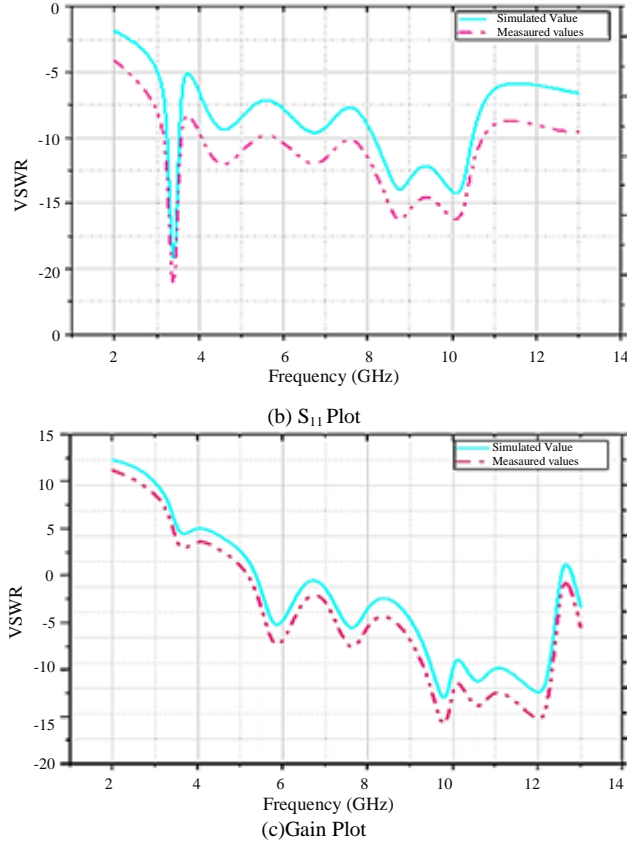


Fig. 14 Simulation and measured values plotting's

Table 5. Performance parameters of both antenna designs

Parameters (Present work done)	Antenna design-1 (Without DRA)	Antenna design-2 (With cylindrical DRA (8x8))
S_{11} (dB)	-15.39	-22.54
Frequency (GHz)	8.9	3.62
VSWR	1.240	1.710
Gain (dB)	-3.059dB	3.44 dB
Polarization (By Axial Ratio)	Linear Polarization at 8.9GHz	Circular Polarization at 3.6GHz

The radiated power is a function of the angular position and the radial distance from the circuit. The variation of power density with angular position is determined by the type and design of the circuit. It can be graphically represented as a radiation pattern. The simulation results of the two designs' radiation patterns are observed below in Figure 9, LHCP and RHCP at 3.6GHz are shown in Figure 10.

7. Antenna Fabrication and Experimental Results Discussion

This section presents the fabricated antenna without DRA and with CDRA (8x8), shown in Figure 11(a, b, and c).The performance characteristics of the fabricated antenna

are verified using a Vector network analyzer, as shown in Figure 12(a, and b). Then fabricated antenna is tested in an anechoic chamber, as shown in Figure 13. Simulated and measured values are shown in Figure 14 (a, b, and c).

8. Conclusion

In this paper, the existing antenna design withoutDRA & Proposed antenna design with CDRA is designed. The simulation results of different sizes of CDRA are analyzed. When comparing the performance parameters of recommended designs. The proposed antenna design with CDRA (8x8) gives better results with a high Gain of around 3.44dB achieved at 3. 6GHz.By using CDRA, circular Polarization is achieved, which yields better image response from the antenna in the applications of GPR.

References:

- [1] Radu Gabriel Pirnău et al., “Ground Penetrating Radars Noninvasive Method used in Soil Science and Archaeology,” *Soil Forming Factors and Processes from the Temperate Zone*, vol. 13, no. 1, pp. 15-31, 2014. [[Google Scholar](#)]
- [2] S. Kundu, and A. Chatterjee, “Sharp Triple-Notched Ultra Wideband Antenna with Gain Augmentation using FSS for Ground Penetrating Radar,” *Wireless Personal Communications*, vol. 117, no. 2, pp. 1399-1418, 2021. [[CrossRef](#)][[Google Scholar](#)][[Publisher Link](#)]
- [3] G. Bit-Babik, C. Di Nallo, and A. Faraone, “Multimode Dielectric Resonator Antenna of Very High Permittivity,” *IEEE Antennas and Propagation Society Symposium*, Monterey, CA, USA, vol. 2, pp. 1383-1386, 2004. [[CrossRef](#)][[Google Scholar](#)][[Publisher Link](#)]
- [4] Harry M. Jol, “Ground Penetrating Radar: Theory and Applications,” Elsevier, Oxford, UK, 2009. [[Google Scholar](#)][[Publisher Link](#)]
- [5] S. Peng, and H. Zheng, “Design of Coplanar- Waveguide-Feed Antenna,” *Structure*, vol. 4, no. 1, 2015. [[Google Scholar](#)]
- [6] Nima Ahmadian, Sayeh Hasan, and Om Prakash Narayan Calla, “Permittivity and Backscattering Coefficient of Diesel Oil Contaminated Soil at C Band (5.3 GHz),” *International Journal of Microwave Science and Technology*, vol. 2013, pp. 1-9, 2013. [[CrossRef](#)][[Google Scholar](#)][[Publisher Link](#)]
- [7] Ahmad H. Abdelgwad, and Tarek M. Said, “Measured Dielectric Permittivity of Contaminated Sandy Soil at Microwave Frequency,” *Journal of Microwaves, Optoelectronics and Electromagnetic Applications*, vol. 15, no. 2, pp. 115-122, 2016. [[CrossRef](#)][[Google Scholar](#)][[Publisher Link](#)]
- [8] Ovidiu Gabriel Avadanei, “Superior Modes in High Permittivity Cylindrical Dielectric Resonator Antenna Excited by a Central Rectangular Slot,” *IEEE Transactions on Antennas and Propagation*, vol. 60, no. 11, pp. 5032-5038, 2012. [[CrossRef](#)][[Google Scholar](#)][[Publisher Link](#)]
- [9] X. L. Travassos et al., “A Review of Ground Penetrating Radar Antenna Design and Optimization,” *Journal of Microwaves, Optoelectronics and Electromagnetic Applications*, vol. 17, no. 3, pp. 385-402, 2018. [[CrossRef](#)][[Google Scholar](#)][[Publisher Link](#)]
- [10] M. B. Oliver, R. K. Mongia, and Y. M. M. Antar, “A New Broadband Circularly Polarized Dielectric Resonator Antenna,” *IEEE Antennas and Propagation Society International Symposium, Digest*, vol. 1, pp. 738-741, 1995. [[CrossRef](#)][[Google Scholar](#)][[Publisher Link](#)]
- [11] S. Fakhte, H. Oraizi and L. Matekovits, “High Gain Rectangular Dielectric Resonator Antenna using Uniaxial Material at Fundamental Mode,” *IEEE Transactions on Antennas and Propagation*, vol. 65, no. 1, pp. 342-347, 2017. [[CrossRef](#)][[Google Scholar](#)][[Publisher Link](#)]
- [12] A. U. Bhoje et al., “Coplanar Waveguide Fed Wide Band Slot Antenna,” *Electronics Letters*, vol. 36, no. 16, pp. 1340-1342, 2000. [[CrossRef](#)][[Google Scholar](#)][[Publisher Link](#)]
- [13] Sounik Kiran Kumar Dash, Taimoor Khan, and Asok De, “Dielectric Resonator Antennas: An Application-Oriented Survey,” *International Journal of RF and Microwave Computer-Aided Engineering*, vol. 27, no. 3, pp. e21069, 2017. [[CrossRef](#)][[Google Scholar](#)][[Publisher Link](#)]
- [14] Xiyao Liu et al., “An Electrically Controlled Pattern and Polarization-Reconfigurable Cylindrical Dielectric Resonator Antenna,” *IEEE Antennas and Wireless Propagation Letters*, vol. 20, no. 12, pp. 2309-2313, 2021. [[CrossRef](#)][[Google Scholar](#)][[Publisher Link](#)]
- [15] Sarah Elgiddawy, “Compact Reconfigurable Polarization Plasma Square Microstrip Patch MIMO Antenna for 5G Wireless Applications,” *2021 38th National Radio Science Conference (NRSC)*, Mansoura, Egypt, pp. 88-95, 2021. [[CrossRef](#)][[Google Scholar](#)][[Publisher Link](#)]
- [16] P. Senthil, M. Suganya, and S. S. Inakshi, “Improve Multidimensional 5G OFDM Based MIMO Sushisen Algorithms Merge Multi-Cell Transmission,” *International Journal of Recent Engineering Science*, vol. 7, no. 2, pp. 17-21, 2020. [[CrossRef](#)][[Google Scholar](#)][[Publisher Link](#)]
- [17] Fu-Ren Hsiao et al., “A Broad Band Very-High-Permittivity Dielectric Resonator Antenna for WLAN Application in the 5.2 GHz Band,” *Microwave and Optical Technology Letters*, vol. 32, no. 6, pp. 426-427, 2002. [[CrossRef](#)][[Google Scholar](#)][[Publisher Link](#)]
- [18] Muath J. Al-Hasan, Tayeb A. Denidni, and Abdel Razik Sebak, “Millimeter Wave EBG-Based Aperture-Coupled Dielectric Resonator Antenna,” *IEEE Transactions on Antennas and Propagation*, vol. 61, no. 8, pp. 4354-4357, 2013. [[CrossRef](#)][[Google Scholar](#)][[Publisher Link](#)]
- [19] Xiyao Liu, Kwok Wa Leung, and Nan Yang, “Wideband Horizontally Polarized Omni directional Cylindrical Dielectric Resonator Antenna for Polarization- Reconfigurable Design,” *IEEE Transactions on Antennas and Propagation*, vol. 69, no. 11, pp. 7333-7342, 2021. [[CrossRef](#)][[Google Scholar](#)][[Publisher Link](#)]
- [20] Jian Ren, Lei Guo, and Kwok Wa Leung, “Wideband Circularly Polarized Cylindrical Dielectric Resonator Antenna,” *IEEE International Symposium on Antennas and Propagation and USNC/URSI National Radio Science Meeting*, San Diego, CA, pp. 1531-1532, 2017. [[CrossRef](#)][[Google Scholar](#)][[Publisher Link](#)]
- [21] Rakesh Chowdhury et al., “Analysis of a Wideband Circularly Polarized Cylindrical Dielectric Resonator Antenna with Broadside Radiation Coupled with Simple Micro Strip Feeding,” *IEEE Access*, vol. 5, pp. 19478-19485, 2017. [[CrossRef](#)][[Google Scholar](#)][[Publisher Link](#)]

- [22] Anuj Kumar Ojha, and A. V. Praveen Kumar, "High Gain Broadside Mode Operation of A Cylindrical Dielectric Resonator Antenna using Simple Slot Excitation," *International Journal of Microwave and Wireless Technologies*, vol. 13, no. 3, pp. 286-294, 2020. [[CrossRef](#)][[Google Scholar](#)][[Publisher Link](#)]
- [23] Chainarong Kittiyapunya, and Monai Krairiksh, "Object Detection of Ground-Penetrating Radar in the Frequency Domain using Three-Antenna System," *IEEE Transactions on Antennas and Propagation*, vol. 70, no. 5, pp. 3672-3679, 2022. [[CrossRef](#)][[Google Scholar](#)][[Publisher Link](#)]
- [24] Tilak Sarmah, Pranjal Borah, and Tulshi Bezboruah, "Tuning of Microstrip Patch Antenna by Adding an Extra Portion at the Upper End of the Antenna," *International Journal of Engineering Trends and Technology*, vol. 71, no. 4, pp. 474-482, 2023. [[CrossRef](#)][[Google Scholar](#)][[Publisher Link](#)]
- [25] Ali Hanafiah Rambe et al., "Design and Simulation of a Rectangular Micro Strip Patch Antenna with a Single Stub for GPR Applications at 500 MHz," *In IOP Conference Series: Materials Science and Engineering*, vol. 1122, no. 1, pp. 012040, 2021. [[CrossRef](#)][[Google Scholar](#)][[Publisher Link](#)]
- [26] M. Firoz Ahmed, M. Hasnat Kabir, and Abu Zafor Md. Touhidul Islam, "Impact of Triangular-Rectangular Slots in the Patch and Partial Ground Plane on Rectangular Patch UWB Antenna Bandwidth Performance," *SSRG International Journal of Recent Engineering Science*, vol. 8, no. 5, pp. 27-31, 2021. [[CrossRef](#)][[Google Scholar](#)][[Publisher Link](#)]
- [27] Zahid Ali et al., "Impact of Ultra-Wideband Antenna Application on Underground Object Detection," *International Journal of Advanced Trends in Computer Science and Engineering*, vol. 10, no. 3, pp. 2441-2446, 2021. [[CrossRef](#)][[Google Scholar](#)][[Publisher Link](#)]
- [28] M. Firoz Ahmed, Abu Zafor Md. Touhidul Islam, and M. Hasnat Kabir, "Design of an Ultra-Wideband Rectangular Patch Microstrip Antenna with Improved Bandwidth," *International Journal of Recent Engineering Science*, vol. 8, no. 5, pp. 6-12, 2021. [[CrossRef](#)][[Google Scholar](#)][[Publisher Link](#)]
- [29] Hai-Han Sun et al., "Compact Dual-Polarized Vivaldi Antenna with High Gain and High Polarization Purity for GPR Applications," *Sensors*, vol. 21, no. 2, pp. 1-17, 2021. [[CrossRef](#)][[Google Scholar](#)][[Publisher Link](#)]